

# MIXER: Multiattribute, Multiway Fusion of Uncertain Pairwise Affinities

Parker C. Lusk, Kaveh Fathian, Jonathan P. How

**Abstract**—We present a multiway fusion algorithm capable of directly processing uncertain pairwise affinities. In contrast to existing works that require initial pairwise *associations*, our MIXER algorithm improves accuracy by leveraging the additional information provided by pairwise affinities. Our main contribution is a multiway fusion formulation that is particularly suited to processing non-binary affinities and a novel continuous relaxation whose solutions are *guaranteed* to be binary, thus avoiding the typical, but potentially problematic, solution binarization steps that may cause infeasibility. A crucial insight of our formulation is that it allows for three modes of association, ranging from non-match, undecided, and match. Exploiting this insight allows fusion to be delayed for some data pairs until more information is available, which is an effective feature for fusion of data with multiple attributes/information sources. We evaluate MIXER on typical synthetic data and benchmark datasets and show increased accuracy against the state of the art in multiway matching, especially in noisy regimes with low observation redundancy. Additionally, we collect RGB data of cars in a parking lot to demonstrate MIXER’s ability to fuse data having multiple attributes (color, visual appearance, and bounding box). On this challenging dataset, MIXER achieves 74%  $F_1$  accuracy and is 49x faster than the next best algorithm, which has 42% accuracy.

## I. INTRODUCTION

Establishing correspondences among data is a fundamental step in many computer vision, robotic perception, and estimation tasks. For example, in structure from motion, SLAM, and object tracking, feature/object matches between sensor observations are desired so that motion can be estimated and landmark maps can be built. Often, pairwise correspondences are identified by solving a linear assignment problem (LAP) after constructing a matrix of feature similarities. In practice, observations are contaminated with noise and false detections that can cause the LAP, typically solved with the Hungarian [1] algorithm, to produce incorrect matches (outliers). When fusing observations from different views or times (e.g., map fusion in SLAM [2]), these outlier matches may cause distinct data to be combined, resulting in inconsistencies [3].

Multiway matching attempts to correct outliers by exploiting observation redundancy and enforcing *cycle consistency*—a property stating that the composition of pairwise matchings over cycles must be identity. Many state-of-the-art multiway matching algorithms do this by permutation synchronization [3]–[12] of pairwise correspondences, which are improved and made consistent by joint optimization.

The authors are with the Department of Aeronautics and Astronautics, Massachusetts Institute of Technology. {plusk, kavehf, jhow}@mit.edu.

This work is supported by the Ford Motor Company, and ARL DCIST under Cooperative Agreement W911NF-17-2-0181.

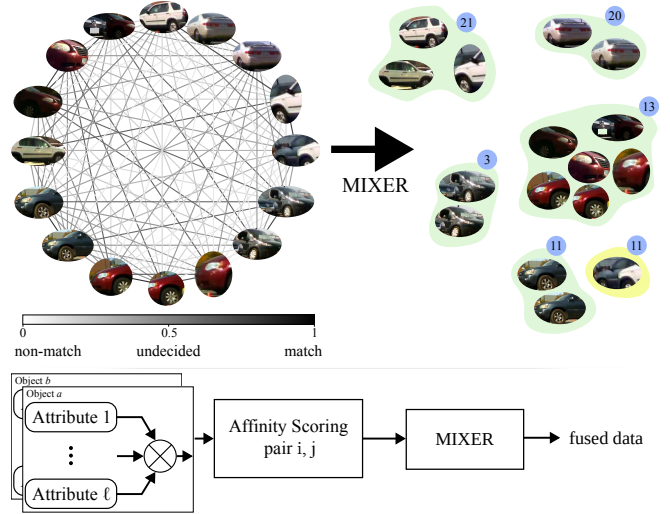


Fig. 1. Multiattribute, multiway fusion example of car detections from different images. Each detection has SIFT, color, and bounding box attributes used to perform pairwise affinity scoring. Pairwise affinities are frequently uncertain, due to noisy detections and scoring processes, and the resulting multiway affinity matrix (graph representation, top left) is inconsistent. Leveraging cycle consistency, distinctness constraints, and three modes of association, MIXER achieves high accuracy data fusion, correctly clustering identical cars (green clusters, top right). If observations are too uncertain, MIXER tends to sacrifice recall in favor of precision, illustrated in the case of car 11—the detection in the yellow cluster is too ambiguous to be fused.

These methods are effective at multiway matching when binary matchings are available; however, their use of (partial) permutation matrices is akin to late fusion [13], [14] and precludes them from using all available information, i.e., multiway matching is performed *after* each pairwise affinity matrix is pre-processed to create binary pairwise matches.

In contrast, we present MIXER (Multiway affinity matrIX fuser), an algorithm that produces cycle consistent multiway matches directly from noisy and uncertain pairwise affinities, i.e., in an early fusion sense. Similar to the conclusions of data fusion works in other contexts [13], [14], our experiments show that MIXER’s early multiway fusion can yield a significant performance increase over existing late fusion approaches. Specifically, direct access to affinities enables a key property of our optimization formulation of multiway fusion. Because of our squared Frobenius objective, our formulation gives rise to three modes of association: non-match, uncertain match, and match, corresponding to 0, 0.5, and 1 affinities, respectively. These three modes also appear in a generalization of pairwise LAP called maximum-weight matching (MWM) [15], [16], where affinities less than or equal to a threshold (i.e., 0.5) will never be associated because they penalize the objective. MIXER extends these ideas

to the multiway case (see Remark 1), balancing the three association modes in conjunction with cycle consistency and other problem constraints to achieve high accuracy in the presence of uncertain pairwise affinity scores. The MIXER pipeline and a fusion example are shown in Fig. 1.

The availability of three association modes is especially important when working with data having multiple modalities or attributes (e.g., color, lidar reflectance, position, bag-of-words vector [17], SIFT descriptors [18], bounding box [19], shape [20], reID features [21], etc.). Because attributes may produce affinity scores in contention (e.g., an object viewed from different viewpoints may have the same color, but not have bounding box overlap), the combined affinity becomes more uncertain, trending toward 0.5. This allows MIXER to defer to other pairwise affinities, and to the problem constraints, before making a decision.

We formulate the early multiway fusion problem as a mixed-integer quadratic program (MIQP). Since the MIQP is not scalable for problem sizes of interest, we propose a novel continuous relaxation leading to approximate solutions. The main contribution of the MIXER algorithm over similar techniques is that its solutions are *guaranteed* to converge to feasible (binary) solutions of the original MIQP. Thus, rounding/projecting results to binary values—which is required when using other techniques and may lead to infeasible solutions—is avoided. To solve the relaxed problem efficiently, we present a projected gradient descent algorithm with backtracking line search. This polynomial-time algorithm has worst case cubic complexity in problem size (from matrix-vector multiplies) at each iteration, and is guaranteed to converge to a stationary point [22, Prop. 7].

We evaluate MIXER on synthetic and real-world datasets and compare the results with state-of-the-art multiway data association algorithms. Our synthetic analysis shows an empirically tight optimality gap of MIXER solutions with respect to the global minimum of the MIQP, while achieving an average runtime of 8 ms—four orders of magnitude faster than solving the MIQP with a general-purpose solver. Our real-world evaluation considers nine multiway matching benchmark datasets, showing that even in the *single* attribute early fusion setting, MIXER is able to achieve high accuracy, superior to the state of the art. Finally, we collect our own dataset of RGB images recorded in a parking lot and attempt to fuse observations of cars seen from multiple viewpoints. Three complementary attributes of cars are extracted (bounding box, color, and SIFT visual appearance) and we show that MIXER significantly outperforms existing algorithms, increasing  $F_1$  score over the next-best result by 32% while being 49x faster. In summary, our main contributions are:

- A principled formulation of multiway fusion as an MIQP that when approached in an early fusion framework leads to three states of association and a multiway extension of the pairwise MWM problem.
- A novel continuous relaxation of the multiway fusion MIQP leading to MIXER, a polynomial-time algorithm based on projected gradient descent that converges to stationary points.

- Theoretical analysis of the continuous relaxation, showing that the MIXER algorithm is guaranteed to converge to feasible, binary solutions of the original MIQP.
- Substantial accuracy and timing improvements over state-of-the-art multiway matching algorithms on standard benchmarks and in a challenging, self-collected RGB dataset with three distinct attributes.

## A. Related Work

**Pairwise association.** Associating elements from two sets based on inter-element similarity scores is traditionally formulated as a LAP [23], which can be optimally solved in polynomial time using, e.g., the Hungarian [1] algorithm. The Hungarian algorithm produces *perfect matchings* (one-to-one correspondence with all elements matched) for *balanced* matching problems (same number of elements in both sets). Imperfect (one-to-one correspondence, all items need not be matched) or unbalanced matching problems can be reduced to perfect, balanced matching to be solved with Hungarian [15]. The case where an imperfect matching of any size is sought that maximizes the possible benefit is called the maximum-weight matching (MWM) problem [16].

If elements have underlying structure (e.g., geometric structure of 3D point clouds) that should be included in the association decision, the problem can be formulated as a quadratic assignment problem [24] (equivalently, graph matching [25]). Unlike the LAP, quadratic assignment (and its equivalent graph matching formulation) is, in general, NP-hard [26]. Generalizations of graph matching introduce additional clique constraints to improve robustness [27].

**Multiway association.** Multiway data association frameworks jointly associate elements across multiple sets to ensure cycle consistency of associations. Multiway association can be formulated as a permutation synchronization problem [4], which is computationally challenging due to its binary domain. With the exception of expensive combinatorial methods [28], [29], existing works consider relaxations to obtain approximate answers. These approximations include spectral relaxation [4], [6], convex relaxation [5], [7], [9], [30], [31], matrix factorization [8], [10], [32], filtering by cluster-consistency statistics [11], message passing [12], and graph clustering [3], [33]–[35]. With the exception of [32], [34], most of the aforementioned methods were originally designed with permutation synchronization in mind and test only with binary associations as input, i.e., in a late fusion approach. Additionally, while our MIQP formulation has been used before [9], [10], our particular relaxation allows us to guarantee that MIXER will converge to feasible, binary solutions, avoiding the final rounding procedure necessary in other works. Lastly, when data points have underlying structure that can be incorporated in the association, the formulation becomes a multi-graph matching problem [33], [36]–[38], which is considerably more computationally challenging.

## II. PROBLEM FORMULATION

In this section, we formalize a principled framework to solve the multiway fusion problem. Consider  $n$  sets of data  $\mathcal{S}_i$ ,  $i = 1, \dots, n$ , with cardinality  $|\mathcal{S}_i| = m_i$  and let  $m = \sum_{i=1}^n m_i$ . We define the *universe* as  $\mathcal{U} \stackrel{\text{def}}{=} \cup_i \mathcal{S}_i$ , with  $|\mathcal{U}| = k \leq m$  distinct elements across all sets. For example, Fig. 2 shows  $n = 3$  images, each with  $m_i$  car detections with bounding box attributes. These are denoted by  $\mathcal{S}_1 \stackrel{\text{def}}{=} \{a, b, c\}$ ,  $\mathcal{S}_2 \stackrel{\text{def}}{=} \{d, e\}$ , and  $\mathcal{S}_3 \stackrel{\text{def}}{=} \{f\}$ . Assuming that we know observations  $a, d, f$  and  $b, e$  represent the same cars, the universe is  $\mathcal{U} \stackrel{\text{def}}{=} \{a, b, c\}$  and has  $k = 3$  elements.

Given two sets  $\mathcal{S}_i$  and  $\mathcal{S}_j$ , we define the *pairwise affinity matrix* between observations as

$$S_{ij} \stackrel{\text{def}}{=} \begin{bmatrix} s_{11} & \cdots & s_{1m_j} \\ \vdots & \ddots & \vdots \\ s_{m_i 1} & \cdots & s_{m_i m_j} \end{bmatrix} \in [0, 1]^{m_i \times m_j}, \quad (1)$$

where  $s_{ab} \in [0, 1]$  denotes the similarity between elements  $a \in \mathcal{S}_i$  and  $b \in \mathcal{S}_j$ . Scores of 0, 0.5, and 1 correspond to maximum dissimilarity, maximum uncertainty/no preference, and maximum similarity, respectively. The *multiway affinity matrix* between all sets is defined as the symmetric matrix

$$S \stackrel{\text{def}}{=} \begin{bmatrix} S_{11} & \cdots & S_{1n} \\ \vdots & \ddots & \vdots \\ S_{n1} & \cdots & S_{nn} \end{bmatrix} \in [0, 1]^{m \times m}, \quad (2)$$

where, by definition,  $S_{ij} = S_{ji}^\top$ . The example in Fig. 2 shows the multiway affinity matrix  $S$  (henceforth called the affinity matrix for simplicity), where  $m = 6$ . Pairwise association matrix blocks are separated by dashed lines.

**Ground-truth association.** The ground-truth pairwise affinity matrices take values of 1 for identical objects and 0 otherwise. When affinity matrices are binary, like in the ground truth case, we refer to them as association matrices. Furthermore, the ground-truth multiway association matrix, denoted by  $A^*$ , can be factorized as  $A^* = UU^\top$ , with the *universal association matrix*  $U$  is defined as

$$U \stackrel{\text{def}}{=} [U_1 \quad \cdots \quad U_n] \in \{0, 1\}^{m \times k}. \quad (3)$$

Matrices  $U_i \in \{0, 1\}^{m_i \times k}$  represent associations between elements of sets  $\mathcal{S}_i$  and  $\mathcal{U}$ . Fig. 2 shows  $A^*$  and  $U$  for the corresponding example, with  $k = 3$  unique cars across all images and where matrices  $U_i$  are separated by dashed lines.

**Constraints.** Often, data association algorithms must meet certain constraints imposed by the high-level task. The *one-to-one* constraint states that an object can be associated with at most one other object. This constraint is satisfied if each row of  $U$  has a single 1 entry. The *distinctness* constraint states that objects within a set are distinct and therefore should not be associated. This is satisfied if there is at most a single 1 entry in each column of  $U_i$ . When the association problem is solved across more than two sets, associations must be *cycle consistent*, that is, if  $a \sim b$ , and  $b \sim c$ , then  $a \sim c$ . This condition is satisfied if the association matrix can be factorized as  $A = UU^\top$  [32]. These three constraints are crucial for detecting and correcting erroneous

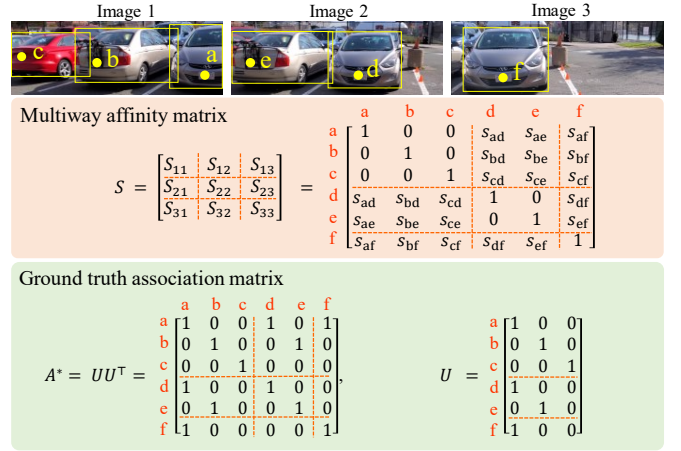


Fig. 2. Example with  $k = 3$  cars across  $n = 3$  images, with a total of  $m = 6$  observations. Bounding box overlap (had they been drawn on the same image) gives the similarity score between two cars. The multiway affinity matrix  $S$  and its corresponding ground truth  $A^*$  are shown.

similarity scores and associations, but increase the difficulty and complexity of the data association procedure.

**Optimization problem.** Given noisy and potentially incorrect similarity scores, our goal is to rectify their values to binary scores that respect the one-to-one, distinctness, and cycle consistency constraints. This goal can be formally stated as finding  $U$  that solves the MIQP

$$\begin{aligned} & \underset{U \in \{0, 1\}^{m \times k}}{\text{minimize}} && \|UU^\top - S\|_F^2 && (\text{cycle consistency}) \\ & \text{subject to} && U\mathbf{1}_m = \mathbf{1}_m && (\text{one-to-one}) \\ & && U_i^\top \mathbf{1}_{m_i} \leq \mathbf{1}_{m_i} && (\text{distinctness}) \end{aligned} \quad (4)$$

where  $\|\cdot\|_F$  is the matrix Frobenius norm and  $\mathbf{1}$  denotes the vector of all ones (with size shown as subscript). When the universe size  $k$  is known (or a good estimate  $\hat{k}$  is available), this can be used directly in (4) to determine the dimensions of  $U$ . However,  $k$  is rarely known in practice and can be difficult to reliably estimate, so instead we allow the algorithm to simultaneously estimate  $U$  and  $k$  by setting  $k = m$ . Then, a solution  $U$  of (4) will have  $\hat{k}$  nonzero columns, giving an estimate of the universe size.

**Remark 1 (Multiway MWM).** For  $n = 2$ , problem (4) reduces to a LAP. Replacing the affinity matrix by  $S \leftarrow \frac{1}{2}(\mathbf{1} - S)$ , problem (4) returns a perfect matching and solutions are equivalent to Hungarian solutions. With  $S$  as specified in Sec. II, (4) solves the MWM problem [16] and can return imperfect matchings. This generalization of the LAP is often more natural for data association since not all data should always be fused.

The traditional two-way MWM problem is often reduced so that a perfect matching exists [15] and is solved using the Hungarian algorithm. This is done by setting any affinity below a threshold to 0 and then discarding any match with 0 affinity in post-processing. Instead, (4) does not require this explicit thresholding and extends to  $n > 2$ , solving the multiway maximum-weight matching problem by allowing the information from multiple pairs of views to inform the final decision.

TABLE I. Comparison of our MIXER formulation with multiway matching algorithms that also relax combinatorial problems with a Frobenius objective. The resulting relaxations are similar, but MIXER guarantees that solutions are cycle consistent (cyc.), distinct (dis.), and binary (bin.). Further, MIXER obtains solution using an efficient projected gradient descent (PGD) method where the projection  $\Pi_{\mathcal{C}}$  onto the constraint set  $\mathcal{C}$  can be evaluated in closed form. When a binary solution is not guaranteed, superscripts ‘c’, ‘t’, and ‘h’ indicate rounding via clustering, thresholding, and Hungarian, respectively. Parameters  $\lambda$  and  $\alpha$  arise due to sparsity regularization (different from our perspective) and are set to the defaults suggested by the respective authors.

Algorithm	Objective	Constraint Set	Solution Method	$\Pi_{\mathcal{C}}(\cdot)$	Soln. Guarantees		
					cyc.	dis.	bin.
MatchLift [5]	minimize $\langle A, \mathbf{1} - \frac{1}{\lambda} S \rangle$ $A \in \mathbb{R}_+^{m \times m}$	$A_{ii} = I_{m_i}, \forall i, \begin{bmatrix} k & \mathbf{1}^\top \\ \mathbf{1} & A \end{bmatrix} \succeq \mathbf{0}$	SDP/ADMM	–	✓	✓	✗ <sup>c</sup>
MatchALS [32]	minimize $\langle A, \mathbf{1} - \frac{1}{\alpha} S \rangle + \lambda \ A\ _*$ $A \in \mathbb{R}_+^{m \times m}$	$A_{ii} = I_{m_i}, \forall i, A_{ij} = A_{ji}^\top, \forall i \neq j$ $\mathbf{0} \leq A_{ij} \mathbf{1} \leq \mathbf{1}, \mathbf{0} \leq A_{ij}^\top \mathbf{1} \leq \mathbf{1}$	ADMM	LP	✗	✓	✗ <sup>t</sup>
MatchDGD [9]	minimize $\langle UU^\top, \mathbf{1} - 2S \rangle + \sum_i \ I - U_i U_i^\top\ _F^2$ $U \in \mathbb{R}_+^{m \times k}$	$U\mathbf{1} = \mathbf{1}, U_i^\top \mathbf{1} \leq \mathbf{1}, \forall i$	PGD	ADMM	✓	✓	✗ <sup>h</sup>
MatchRTR [10]	minimize $\langle UU^\top, \mathbf{1} - 2S \rangle + \sum_i \ I - U_i U_i^\top\ _F^2$ $U \in \mathbb{R}_+^{m \times k}$	$U\mathbf{1} = \mathbf{1}$	Riemannian trust-region	closed form	✓	✗	✗ <sup>h</sup>
MIXER	minimize $\langle UU^\top, \mathbf{1} - 2S \rangle + d(\phi_{\text{orth}}(U) + \phi_{\text{dist}}(U))$ $U \in \mathbb{R}_+^{m \times m}$	$U\mathbf{1} = \mathbf{1}$	PGD	closed form	✓	✓	✓

### III. CONTINUOUS RELAXATION AND ALGORITHM

Due to its binary domain, solving (4) to global optimality requires combinatorial techniques that quickly become intractable as the problem size grows. To increase scalability, the standard workaround is to relax the domain of the problem to the positive orthant. However, these solutions must be subsequently *rounded* (i.e., projected back to binary values), which can be problematic since this may produce infeasible solutions that violate the original constraints. A key novelty of our relaxation approach and algorithm is that solutions are *guaranteed* to converge to *feasible, binary* solutions of the original problem (4), thereby obviating the potentially problematic rounding step. Towards our relaxation and guarantees, we state the following equivalent formulation of (4)

$$\begin{aligned}
& \text{minimize}_{U \in \{0,1\}^{m \times m}} \langle UU^\top, \mathbf{1} - 2S \rangle && \text{(cycle consistency)} \\
& \text{subject to} && U \in \Delta^{m \times m} && \text{(one-to-one constraint)} \\
& && \phi_{\text{orth}}(U) = 0 && \text{(orthogonality constraint)} \\
& && \phi_{\text{dist}}(U) = 0 && \text{(distinctness constraint)}
\end{aligned} \tag{5}$$

where  $\Delta^{m \times m} \stackrel{\text{def}}{=} \{U \in \mathbb{R}_+^{m \times m} : U\mathbf{1}_m = \mathbf{1}_m\}$  is the (matrix) standard simplex and  $\phi_{\text{orth}}, \phi_{\text{dist}}$  are the penalty functions

$$\phi_{\text{orth}} \stackrel{\text{def}}{=} \langle U^\top U, P_o \rangle, \quad \phi_{\text{dist}} \stackrel{\text{def}}{=} \langle UU^\top, P_d \rangle, \tag{6}$$

with penalty matrices defined as  $P_o \stackrel{\text{def}}{=} \mathbf{1} - I$  and  $P_d \stackrel{\text{def}}{=} \text{blockdiag}(P_{d1}, \dots, P_{dn})$ , and  $P_{di} \stackrel{\text{def}}{=} \mathbf{1}_{m_i \times m_i} - I_{m_i \times m_i}$ . The following lemmas shed light on these penalty functions.

**Lemma 1.** *A matrix  $U \in \Delta^{m \times m}$  is binary if and only if the columns of  $U$  are orthogonal.*

**Lemma 2.** *Given  $U \in \{0,1\}^{m \times m}$  and  $\phi_{\text{dist}}(U)$  as defined,  $\phi_{\text{dist}}(U) = 0$  if and only if  $U_i^\top \mathbf{1}_{m_i} \leq \mathbf{1}_{m_i}$ .*

Lemma 1 indicates that column orthogonality of  $U$  is an implicit constraint in the MIQP (4) due to the binary domain.

Using this insight, a penalty function for orthogonality is constructed and added to the equivalent formulation in (5). Lemma 2 states the equivalence of the distinctness constraint with the penalty function  $\phi_{\text{dist}}$ , which is also added to (5). Detailed proofs of these lemmas and of the equivalence between (5) and (4) are given in [39, Appendix I].

**Relaxed Formulation.** We relax problem (5) as

$$\begin{aligned}
& \text{minimize}_U \quad F(U) \stackrel{\text{def}}{=} \langle UU^\top, \mathbf{1} - 2S \rangle \\
& \quad \quad \quad + d(\phi_{\text{orth}}(U) + \phi_{\text{dist}}(U)) \\
& \text{subject to} \quad U \in \Delta^{m \times m}
\end{aligned} \tag{7}$$

We approach solving (7) by gradually increasing the scalar parameter  $d \geq 0$ . The rationale is that the affinity  $S$  is indicative of the ground truth and so an initially small  $d$  allows  $U$  to be biased towards a good solution, while a large  $d$  ultimately pushes the solution  $U$  towards a feasible, binary stationary point. However, note that (7) is a non-linear, non-convex problem and so both saddle points and local optima exist. The following results, which follow from analysis of the KKT conditions [40], discuss these stationary points.

**Lemma 3.** *As  $d \rightarrow \infty$ , if a stationary point  $U^* \in \Delta^{m \times m}$  is binary, then  $\phi_{\text{dist}}(U^*) = 0$ , i.e., distinctness is satisfied.*

**Lemma 4.** *As  $d \rightarrow \infty$ , if a stationary point  $U^* \in \Delta^{m \times m}$  is non-binary, then  $U^*$  is a saddle point.*

These results allows the detection of non-binary saddle points, which can then be escaped by solving for a feasible descent direction with negative curvature as in [22]. Therefore, by solving (7) with increasing  $d$ , we are guaranteed to achieve a  $U$  that is binary, one-to-one, distinct, and cycle consistent like in (4). Although Lemmas 3 and 4 provide important theoretical insights, taking  $d \rightarrow \infty$  is not algorithmically practical. The following theorem provides a lower bound on  $d$ , after which Lemmas 3 and 4 are valid.

**Theorem 1.** *If  $d \geq m + 1$ , then local minima are binary.*

The proof of Theorem 1 and Lemmas 3 and 4 are given



---

**Algorithm 1** MIXER

---

```
1: Input affinity matrix  $S \in [0, 1]^{m \times m}$ , set cardinalities  $m_i \in \mathbb{N}^n$ 
   (if distinctness is required)
2: Output  $U \in \{0, 1\}^{m \times m}$ 
3:  $U \leftarrow \Pi_{\Delta}(\text{eigvec}(\mathbf{1} - 2S))$  % initialize using eigenvectors
4:  $d \leftarrow d_0$  % initialize d small, default:  $d_0 = 1/\sqrt{m}$ 
5: while  $d < m + 1$  do
6:   while  $U$  not converged do
7:      $\nabla F = 2(\mathbf{1} - 2S)U + 2d(U P_o + P_d U)$ 
8:      $U \leftarrow \Pi_{\Delta}(U - \alpha \nabla F)$  %  $\alpha$  via backtracking line search
9:    $d \leftarrow d + \text{med}\{|\frac{[1-2S]}{[UP_o + P_d U]}| : [UP_o + P_d U] > 0, [U] > 0\}$ 
10:  if  $U$  binary and  $\phi_{\text{dist}}(U) = 0$  then return
```

---

in [39, Appendix I]. For a comparison of our relaxation and its guarantees with existing approaches having similar formulations, see Table I.

**Algorithm.** MIXER is summarized in Algorithm 1. The solution is initialized using the eigenvectors of the modified affinity matrix,  $\mathbf{1} - 2S$  (Line 3). The penalty weight  $d$  is first initialized to a small value (Line 4). For each value of  $d$ , we solve (7) using projected gradient descent (PGD) with the projection  $\Pi_{\Delta}$  onto the convex constraint set. The projection operation can be efficiently implemented as a non-iterative algorithm [41]. PGD over convex constraints is guaranteed to converge to stationary points [22, Prop. 7]. Once  $U$  converges to a stationary point,  $d$  is increased by selecting the median value that leads the gradient at the next step to vanish. Theorem 1, ensures that  $U$  will become binary once  $d \geq m + 1$ . However, in practice we often terminate much sooner than this by checking if  $U$  is binary and distinctness is satisfied.

**Computational complexity.** Neglecting constant factors, the worst-case complexity of Algorithm 1 is bounded by  $\mathcal{O}(m^3)$  per iteration, corresponding to matrix multiplications. We observed that most of the runtime is spent computing the matrix-vector products in  $\nabla F$  and  $F$  and by the  $\mathcal{O}(m^2 \log m)$  projection onto the matrix simplex,  $\Pi_{\Delta}$ .

#### IV. EXPERIMENTS

We evaluate MIXER in three experiments. First, we use synthetic data to validate that our MIQP problem formulation (4) enables high accuracy. We find that MIXER achieves near-optimal performance compared to several existing state-of-the-art multiway matching algorithms. Second, we compare MIXER with other algorithms using standard multiway image feature matching benchmarks. Finally, we apply multiway fusion to a challenging robotics dataset collected as part of this work, highlighting MIXER’s ability to use multiple attributes to improve the overall fusion accuracy.

We report matching accuracy in terms of precision, recall, and the  $F_1$  score. Precision  $p$  is the number of correct associations divided by the total number of associations identified, recall  $r$  is the number of correct associations identified divided by the total number of associations in the ground truth, and the  $F_1$  score is defined as  $\frac{2pr}{p+r} \in [0, 1]$ , which captures the balance between precision and recall.

We compare against several state-of-the-art multiway matching algorithms. Spectral [4] and MatchEig [6] are

based on spectral relaxation, CLEAR [3] and QuickMatch [34] are based on graph clustering, FCC [11] is based on cluster-consistency statistics, NMFSync [8] is based on matrix factorization, MatchALS [32] is based on low-rank matrix recovery, and MatchLift [5] is based on convex relaxation. Except for MIXER, QuickMatch and FCC, algorithms require a universe size estimate and we use CLEAR’s estimate as the typical spectral approach is typically sensitive to noisy affinity matrices [3], [6], [32]. For MatchALS, we scale this estimate by two as suggested by the authors. As a baseline, we perform pairwise data association using Hungarian with a minimum score threshold (0.35), as commonly done in the tracking literature [19], demonstrating the type of noisy, cycle inconsistent results that arise when naively fusing a set of pairwise associations. For algorithms that do not guarantee cycle consistency (baseline, FCC, MatchEig, MatchALS), we complete their solutions into cliques (see [3, §VII]) and denote the result with a “(C)”. For small problems, we globally solve the MIQP (4) to optimality using Gurobi 9.5.2 and refer to this implementation as MIXER\*. All algorithms are implemented in MATLAB and executed on an i7-6700 CPU with 32 GB RAM.

##### A. Synthetic Dataset

In this section, we use Monte Carlo analysis with synthetic data to compare MIXER with several state-of-the-art algorithms across different noise regimes. We aim to 1) validate our formulation (4) for high-accuracy multiway fusion, 2) show the ability of MIXER to obtain near-optimal and thus high-accuracy solutions, 3) show that early fusion with MIXER achieves higher accuracy than late fusion with existing methods, and 4) show that MIXER provides a computationally scalable approach to approximately solve (4). Noisy pairwise associations are synthetically generated by considering  $n = 10$  partial views of  $k = 30$  objects, e.g., 10 images each containing at most 30 objects. Twenty-five different noise regimes are considered, wherein the percent mismatch (i.e., binary noise added to ground truth associations) and the probability of observation (i.e., selection of random subsets of the universe) are varied. A noisy association  $a_{kl}^{ij} \in \{0, 1\}$  of objects  $k$  and  $l$  from views  $i$  and  $j$  is then made into an affinity  $s_{kl}^{ij} \in [0, 1]$  by adding uncertainty according to  $s(a; \theta) = (1 - \theta)a + 0.5\theta$ , where  $\theta$  is drawn from a standard uniform distribution. Each algorithm processes these noisy pairwise affinities, allowing us to study the accuracy of each method as an early fusion approach.

Fig. 3 shows average results over 10 Monte Carlo trials. While all algorithms generally perform well in low noise regimes with perfect observability (top left squares of Fig. 3), the performance of most algorithms quickly deteriorates as the probability of observing objects decreases. MIXER is the exception, performing better than other approaches on average, over the entire range of mismatch and partial observability. The low observation redundancy regimes (bottom rows in Fig. 3) are especially important because these settings occur when limited field-of-view sensors only see portions of the universe; for example, in multirobot SLAM [2], [42].

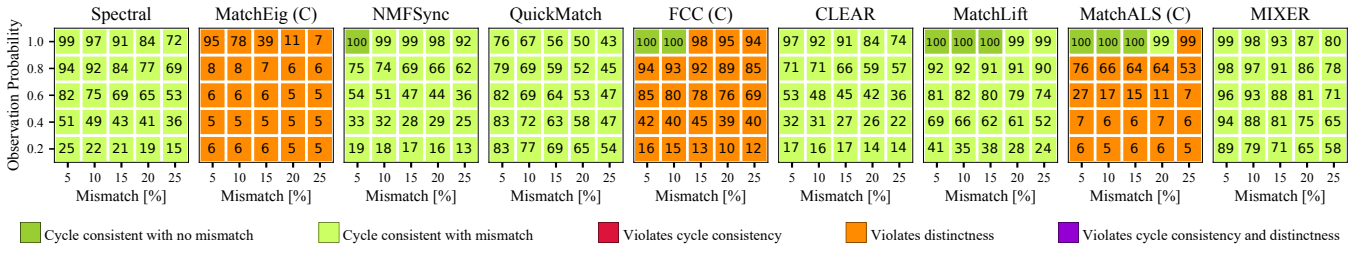


Fig. 3. Multiway early fusion of noisy pairwise affinities generated from  $n = 10$  simulated views of a universe with  $k = 30$  distinct objects. MIXER accurately fuses pairwise affinities while enforcing cycle consistency and distinctness, performing better than the state-of-the-art over the entire range of noise regimes. Especially apparent is the high accuracy of MIXER compared to existing methods in low observation redundancy settings (bottom rows).

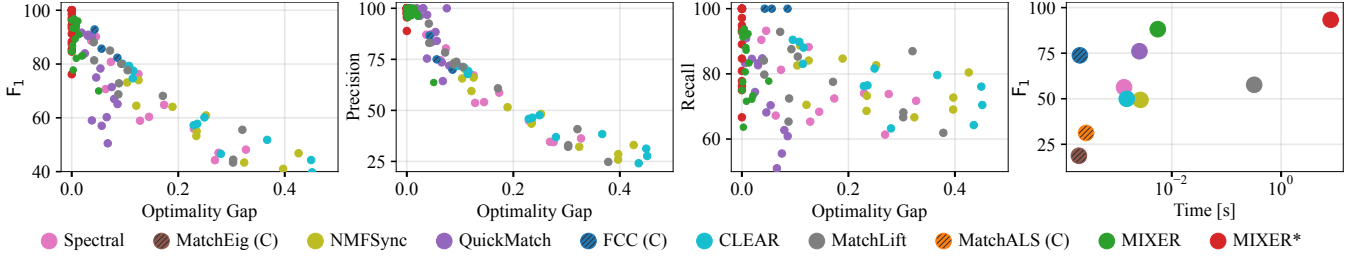


Fig. 4.  $F_1$ , precision, and recall compared with optimality gaps relative to our MIQP formulation (4). Each point corresponds to a solution of a synthetic problem having some observation probability and mismatch percentage (e.g., see Fig. 3). As the optimality gap of a solution decreases, the accuracy increases, validating our multiway fusion formulation. MIXER solutions are tightly grouped in the high-accuracy, near-optimal regime. The last plot visualizes each algorithm’s average accuracy vs runtime, showing that MIXER is much more scalable than directly solving the MIQP.

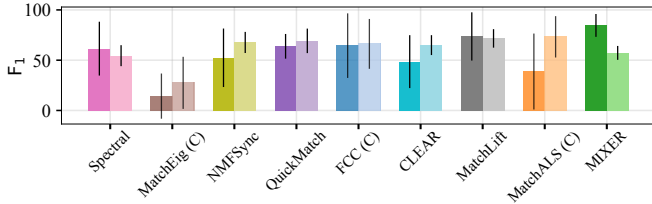


Fig. 5. Average  $F_1$  results using early fusion (left bars) and late fusion (right bars). Note that MatchEig (C) and MatchALS (C) violate distinctness constraints and so these infeasible results are indicated with hatch marks.

To assess how well our formulation (4) addresses the multiway fusion problem, we compute the optimality gap of each algorithm’s solutions compared to MIXER\*. Fig. 4 plots the accuracy of each solution against the optimality gap, exposing the correlation between low optimality gap and high accuracy ( $F_1$  and precision). MIXER solutions are tightly grouped in this near-optimal, high-accuracy regime, showing that our algorithm, although a local, first-order method, is frequently able to achieve good results. Interestingly, we observe in the recall results of Fig. 4 that our formulation leads MIXER to be conservative—it would rather *not* fuse objects if precision would be sacrificed. This property allows further improvements to be made as more data is collected.

Finally, Fig. 5 highlights that early fusion with MIXER outperforms both early and late fusion of uncertain affinities compared to existing state-of-the-art algorithms. In late fusion, pairwise affinities are first processed into hard matches before multiway matching is performed, and in this setting, MIXER does not perform as well. The principal reason is because MIXER is a multiway MWM formulation as discussed in Remark 1—when pairwise associations are first made, a large amount of information is discarded, precluding MIXER from using it in combination with multiway constraints.

## B. Benchmark Datasets

We use the CMU Hotel<sup>1</sup> and Affine Covariant Features<sup>2</sup> benchmark datasets to demonstrate multiway fusion with MIXER on real data and report results in Table II. These datasets consist of collections of images from different perspectives and the goal is to extract features from each image, perform pairwise feature matching, and then perform multiway fusion of features. Instead of standard pairwise SIFT matching, which would cause late fusion since it makes hard decisions about pairwise association and thus limits the ability of multiway fusion to make fully-informed decisions, we instead construct pairwise affinity matrices using k-nearest neighbors. Pairwise affinities are created by finding the 10 closest SIFT matches ( $\ell_1$  distance) for each keypoint. The affinity score of the closest neighbor is set to 1, the other neighbors set to 0.5, and the rest to 0. This makes use of all three states of association and indicates that for the semi-close neighbors, there is some uncertainty as to whether or not they should be matched, while for far away neighbors they are very likely to be incorrect matches.

## C. Car Fusion Dataset

In this section, we evaluate MIXER’s ability to fuse observation of objects seen from multiple views. Multiway object fusion is a task that appears in settings like multirobot SLAM [2], [42] and multimodal object tracking [43]. We collect data by teleoperating a Clearpath Jackal equipped with an RGB camera around a parking lot as shown in Fig. 6. We select  $n = 184$  images from two separate traversals to create large view changes and thus increase the difficulty. In total, there are  $k = 22$  distinct cars

<sup>1</sup><http://pages.cs.wisc.edu/~pachauri/perm-sync/>

<sup>2</sup><https://www.robots.ox.ac.uk/~vgg/data/affine>

TABLE II. Benchmark results on CMU Hotel and Affine Covariant Features datasets.  $F_1$  scores are reported as percentages. Results that violate cycle consistency are indicated in **red** and are completed to assess their true fusion accuracy. When fusing cycle inconsistent solutions, distinctness is often violated and these results are indicated in **orange**. In every case, MatchLift is at least 1 order of magnitude slower than MIXER (see Fig. 4).

Algorithm	Hotel	Wall	UBC	Bikes	Leuven	Trees	Graffiti	Bark	Boat
Baseline	89.2	49.0	71.1	52.4	68.9	44.0	40.9	39.4	47.6
Baseline (C)	16.8	2.2	5.9	1.4	4.9	1.5	0.3	10.7	0.9
Spectral	65.3	43.8	51.5	48.5	58.5	46.2	34.1	31.4	26.8
MatchEig	94.7	78.4	84.4	75.7	78.9	50.4	48.0	37.5	61.2
MatchEig (C)	27.2	16.1	10.8	1.9	4.1	1.6	0.3	4.0	1.1
NMFSync	89.7	39.4	63.2	58.4	59.5	33.5	29.3	18.9	44.1
QuickMatch	82.4	46.4	65.7	50.9	62.7	42.3	39.5	28.2	43.4
FCC	92.5	55.7	77.4	59.0	68.8	51.7	40.4	42.1	32.3
FCC (C)	92.8	46.3	70.8	52.8	58.5	41.0	32.4	30.2	29.9
CLEAR	76.9	40.9	47.8	40.3	53.1	26.1	28.1	25.8	38.9
MatchALS	95.4	71.4	77.1	71.1	73.9	50.8	46.7	38.4	58.7
MatchALS (C)	89.3	43.1	26.4	39.2	39.2	21.9	11.1	26.9	35.0
MatchLift	95.9	55.9	79.2	63.8	71.9	48.2	45.4	35.0	54.4
MIXER	97.0	56.4	77.7	67.5	74.2	51.0	43.3	40.0	59.2

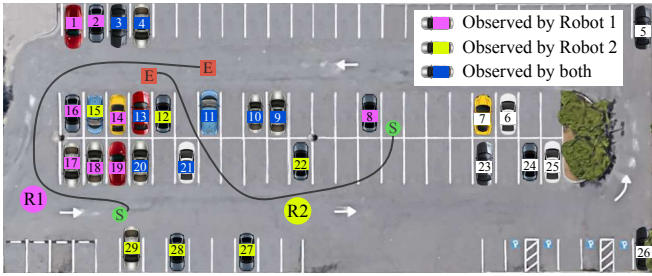


Fig. 6. Illustration of the parking lot dataset, with the paths of two robots (R1 and R2), from start (S) to end (E). The robots observed  $k = 22$  cars, with 8 cars being co-visible. Colors indicate which robot saw which car.

visible from 339 car detections, resulting in only 8% of the universe being observed in each image. Using these RGB images, the objective is to fuse cars seen from different views using noisy, partial, and cropped detections (i.e., not every car is seen in each frame, and some cars extend out of frame). Cars are detected using YOLOv3 [44] and we extract three attributes from each detection: bounding box, car color, and visual appearance. These three attributes have complementary strengths. For example, bounding boxes are good for scoring consecutive detections, but cannot be used over large time offsets; car color is a sensitive quantity to extract, but is good for associating detections over large time offsets; visual appearance based on the number of matching SIFT descriptors is typically robust to small/medium view changes, but breaks down with large view changes. Thus, using these attributes highlights the three-states-of-association feature of the formulation of problem (4), which allows MIXER to achieve high accuracy. Ground truth associations are generated by manually annotating the detections.

Each attribute creates its own set of pairwise affinities, which will be combined to create a single multiway affinity matrix. Bounding box affinity is scored using intersection-over-union (IoU) for consecutive detections, while non-consecutive detections take a value of 0.5 as wide-baseline IoU scoring is inconclusive. Color affinity scores take either 0, 0.5, or 1, with 0.5 being used if either car’s color could not be clearly ascertained. Visual similarity is scored based on the number of SIFT matches between two cars. Com-

TABLE III. Multiway car fusion results. Objective values are listed except for solutions that violate cycle consistency (**red**) or distinctness (**orange**).

Algorithm	Precision	Recall	$F_1$	Obj. ( $\downarrow$ )	Time [ms]
Baseline	44.9	14.8	22.3	—	1648
Baseline (C)	8.2	84.5	14.9	—	1650
Spectral	22.8	58.0	32.7	146.9	12
MatchEig	13.0	72.8	22.1	—	1079
MatchEig (C)	6.3	99.7	11.8	—	1083
NMFSync	15.7	58.6	24.7	151.5	35
QuickMatch	13.8	31.2	19.2	148.9	37
FCC	47.4	70.8	56.8	—	3269
FCC (C)	6.3	98.1	11.9	—	3272
CLEAR	19.0	66.4	29.6	150.6	63
MatchALS	7.5	94.9	13.9	—	542
MatchALS (C)	6.3	99.9	11.8	—	545
MatchLift	12.4	48.8	20.1	149.7	15 463
MatchALS $_{\alpha=0.5}$	41.9	76.7	54.2	—	614
MatchALS $_{\alpha=0.5}$ (C)	8.9	87.6	16.1	—	617
MatchLift $_{\lambda=0.5}$	34.6	54.7	42.4	141.1	15 295
MIXER	79.4	70.6	74.8	135.7	312

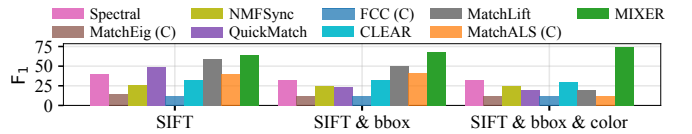


Fig. 7. Multiway car fusion results, incrementally adding additional attribute affinities. Mixing together attributes allows MIXER to increase in  $F_1$  score by more than 10%. In contrast, the combination of additional uncertain information causes other methods to decrease in  $F_1$  accuracy.

mon attribute affinity combination/fusion methods include (weighted) averaging, non-maximum suppression, probabilistic ensembling [45], multi-layer perceptrons [43], graph neural networks [46], or other learned fusion processes [47]. For simplicity, we adopt the weighted averaging approach, using a weights of 1, 0.5, and 1 for bounding box overlap, color similarity, and appearance similarity, respectively. These weights are chosen because of the lack of robustness in color detection and scoring.

In addition to the state-of-the-art algorithms implemented by the respective authors, we also report results for MatchALS $_{\alpha=0.5}$  and MatchLift $_{\lambda=0.5}$  with parameters set so that the input affinity matrix is transformed to  $\mathbf{1} - 2S$  like in MIXER (see Table I). In MatchALS and MatchLift, these parameters—and therefore the coefficient scaling on  $S$ —are heuristically introduced to encourage sparsity, with default values suggested by their authors of  $\alpha = 0.1$  and  $\lambda = \sqrt{\binom{n}{2}}/(2n) \approx 0.3$ , respectively. In contrast, the expression  $\mathbf{1} - 2S$  arises naturally in our formulation due to the Frobenius objective (4) and our insight is that it allows for three states of association in multiway MWM (see Remark 1). Setting  $\alpha = \lambda = 0.5$  allows for a direct comparison of the relaxations and algorithms listed in Table I and, as expected due to our insights, they provide an increase in accuracy. However, as reported in Table III, MIXER substantially outperforms existing algorithms. It is followed by MatchLift $_{\lambda=0.5}$ , which lags by 32% in  $F_1$  accuracy and is 49x slower. Although MatchALS $_{\alpha=0.5}$  and MatchLift $_{\lambda=0.5}$  also have three states of association, their relaxations require rounding to binary matrices and search for solutions in association space  $A \in \mathbb{R}_+^{m \times m}$ , leading to sensitivity of the universe size estimate.

The reason for MIXER’s dominance over the state-of-the-art in this setting is two-fold. First, its ability to attain near-optimal solutions using a scalable PGD method, even in low-redundancy settings (e.g., bottom rows of Fig. 3). Second, accuracy at near-optimal solutions is high because of the MIQP formulation (4), which allows for three states of association and therefore a way to combine uncertain affinities from multiple attributes, as shown in Fig. 7.

## V. CONCLUSION

We presented the MIXER algorithm for multiattribute, multiway fusion of uncertain pairwise affinities. Our MIQP formulation leverages direct access to affinities and allows three modes of association (non-match, undecided, and match) over the range 0 to 1. This feature led to the insight that our formulation is a multiway extension of the maximum-weight matching (MWM) problem (see Remark 1). Because of the binary constraints embedded in the MIQP, we proposed a novel continuous relaxation in a projected gradient descent scheme to converge to feasible, binary solutions of the original problem. The guarantee of our algorithm to converge to binary points sets it apart from related work, which relies on a final binarization step that can lead solutions to be infeasible. Finally, our experimental evaluations in three datasets showed that MIXER frequently achieves higher accuracy than the state of the art, especially in noisy regimes with low observation redundancy. These properties and results establish MIXER as an effective and scalable multiway fusion algorithm in the presence of uncertain affinities.

## REFERENCES

- [1] H. W. Kuhn, “The hungarian method for the assignment problem,” *Naval Research Logistics Quarterly*, vol. 2, no. 1-2, pp. 83–97, 1955.
- [2] R. Aragues, E. Montijano, and C. Sagües, “Consistent data association in multi-robot systems with limited communications,” in *RSS*, 2011.
- [3] K. Fathian, K. Khosoussi, Y. Tian, P. Lusk, and J. P. How, “CLEAR: A consistent lifting, embedding, and alignment rectification algorithm for multiview data association,” *IEEE T-RO*, vol. 36, no. 6, 2020.
- [4] D. Pachauri, R. Kondor, and V. Singh, “Solving the multi-way matching problem by permutation synchronization,” in *NeurIPS*, 2013.
- [5] Y. Chen, L. Guibas, and Q. Huang, “Near-optimal joint object matching via convex relaxation,” in *ICML*, vol. 32, no. 2, 2014, pp. 100–108.
- [6] E. Maset, F. Arrigoni, and A. Fusiello, “Practical and efficient multi-view matching,” in *IEEE ICCV*, 2017, pp. 4578–4586.
- [7] S. Leonardos, X. Zhou, and K. Daniilidis, “Distributed consistent data association via permutation synchronization,” in *IEEE ICRA*, 2017.
- [8] F. Bernard, J. Thunberg, J. Goncalves, and C. Theobalt, “Synchronization of partial multi-matchings via non-negative factorisations,” *Pattern Recognition*, vol. 92, pp. 146–155, 2019.
- [9] S. Leonardos and K. Daniilidis, “A distributed optimization approach to consistent multiway matching,” in *IEEE CDC*, 2018, pp. 89–96.
- [10] S. Leonardos, X. Zhou, and K. Daniilidis, “A low-rank matrix approximation approach to multiway matching with applications in multi-sensory data association,” in *IEEE ICRA*, 2020, pp. 8665–8671.
- [11] Y. Shi, S. Li, T. Maunu, and G. Lerman, “Scalable cluster-consistency statistics for robust multi-object matching,” in *IEEE 3DV*, 2021.
- [12] S. Li, Y. Shi, and G. Lerman, “Fast, accurate and memory-efficient partial permutation synchronization,” in *IEEE/CVF CVPR*, 2022.
- [13] C. G. Snoek, M. Worring, and A. W. Smeulders, “Early versus late fusion in semantic video analysis,” in *ACM Multimedia*, 2005.
- [14] K. Gadzicki, R. Khamsehashari, and C. Zetsche, “Early vs late fusion in multimodal convolutional neural networks,” in *FUSION*, 2020.
- [15] L. Ramshaw and R. E. Tarjan, “On minimum-cost assignments in unbalanced bipartite graphs,” *HP Labs, Palo Alto, CA, USA, Tech. Rep. HPL-2012-40R1*, vol. 20, 2012.
- [16] R. Duan and S. Pettie, “Linear-time approximation for maximum weight matching,” *Journal of the ACM*, vol. 61, no. 1, 2014.
- [17] D. Gálvez-López and J. D. Tardos, “Bags of binary words for fast place recognition in image sequences,” *IEEE T-RO*, 2012.
- [18] D. G. Lowe, “Distinctive image features from scale-invariant keypoints,” *IJCV*, vol. 60, no. 2, pp. 91–110, 2004.
- [19] A. Bewley, Z. Ge, L. Ott, F. Ramos, and B. Upcroft, “Simple online and realtime tracking,” in *IEEE ICIP*, 2016, pp. 3464–3468.
- [20] T. F. Cootes, C. J. Taylor, D. H. Cooper, and J. Graham, “Active shape models-their training and application,” *Computer vision and image understanding*, vol. 61, no. 1, pp. 38–59, 1995.
- [21] S. Karanam, M. Gou, Z. Wu, A. Rates-Borras, O. Camps, and R. J. Radke, “A systematic evaluation and benchmark for person re-identification: Features, metrics, and datasets,” *IEEE TPAMI*, 2019.
- [22] A. Mokhtari, A. Ozdaglar, and A. Jadbabaie, “Escaping saddle points in constrained optimization,” *NeurIPS*, vol. 31, 2018.
- [23] R. Burkard, M. Dell’Amico, and S. Martello, “Assignment problems,” *SIAM*, 2009.
- [24] E. L. Lawler, “The quadratic assignment problem,” *Management science*, vol. 9, no. 4, pp. 586–599, 1963.
- [25] D. Conte, P. Foggia, C. Sansone, and M. Vento, “Thirty years of graph matching in pattern recognition,” *IJPRAI*, vol. 18, no. 3, 2004.
- [26] S. Sahni and T. Gonzalez, “P-complete approximation problems,” *Journal of the ACM*, vol. 23, no. 3, pp. 555–565, 1976.
- [27] P. C. Lusk, K. Fathian, and J. P. How, “CLIPPER: A graph-theoretic framework for robust data association,” in *IEEE ICRA*, 2021.
- [28] C. Zach, M. Klopschitz, and M. Pollefeys, “Disambiguating visual relations using loop constraints,” in *IEEE CVPR*, 2010.
- [29] A. Nguyen, M. Ben-Chen, K. Welnicka, Y. Ye, and L. Guibas, “An optimization approach to improving collections of shape maps,” in *Computer Graphics Forum*, vol. 30, no. 5, 2011, pp. 1481–1491.
- [30] N. Hu, Q. Huang, B. Thibert, and L. J. Guibas, “Distributable consistent multi-object matching,” in *IEEE CVPR*, 2018.
- [31] J.-G. Yu, G.-S. Xia, A. Samal, and J. Tian, “Globally consistent correspondence of multiple feature sets using proximal gauss–seidel relaxation,” *Pattern Recognition*, vol. 51, pp. 255–267, 2016.
- [32] X. Zhou, M. Zhu, and K. Daniilidis, “Multi-image matching via fast alternating minimization,” in *IEEE ICCV*, 2015, pp. 4032–4040.
- [33] J. Yan, M. Cho, H. Zha, X. Yang, and S. M. Chu, “Multi-graph matching via affinity optimization with graduated consistency regularization,” *IEEE TPAMI*, vol. 38, no. 6, pp. 1228–1242, 2015.
- [34] R. Tron, X. Zhou, C. Esteves, and K. Daniilidis, “Fast multi-image matching via density-based clustering,” in *IEEE ICCV*, 2017.
- [35] Z. Serlin, G. Yang, B. Sookraj, C. Belta, and R. Tron, “Distributed and consistent multi-image feature matching via quickmatch,” *IJRR*, vol. 39, no. 10-11, pp. 1222–1238, 2020.
- [36] J. Yan, Y. Tian, H. Zha, X. Yang, Y. Zhang, and S. M. Chu, “Joint optimization for consistent multiple graph matching,” in *IEEE ICCV*, 2013, pp. 1649–1656.
- [37] X. Shi, H. Ling, W. Hu, J. Xing, and Y. Zhang, “Tensor power iteration for multi-graph matching,” in *IEEE CVPR*, 2016, pp. 5062–5070.
- [38] P. Swoboda, D. Kainmuller, A. Mokarian, C. Theobalt, and F. Bernard, “A convex relaxation for multi-graph matching,” in *IEEE CVPR*, 2019.
- [39] P. C. Lusk, K. Fathian, and J. P. How, “MIXER: Multiattribute, Multiway Fusion of Uncertain Data Associations,” 2022, <https://arxiv.org/pdf/2111.14990.pdf>.
- [40] J. Nocedal and S. J. Wright, *Numerical optimization*. Springer, 1999.
- [41] W. Wang and M. A. Carreira-Perpinán, “Projection onto the probability simplex: An efficient algorithm with a simple proof, and an application,” *arXiv preprint arXiv:1309.1541*, 2013.
- [42] Y. Tian, Y. Chang, F. H. Arias, C. Nieto-Granda, J. P. How, and L. Carlone, “Kimera-multi: robust, distributed, dense metric-semantic slam for multi-robot systems,” *IEEE Transactions on Robotics*, 2022.
- [43] H.-k. Chiu, J. Li, R. Ambruş, and J. Bohg, “Probabilistic 3d multi-modal, multi-object tracking for autonomous driving,” in *IEEE ICRA*, 2021, pp. 14 227–14 233.
- [44] J. Redmon and A. Farhadi, “YOLOv3: An Incremental Improvement,” *arXiv*, 2018.
- [45] Y.-T. Chen, J. Shi, C. Mertz, S. Kong, and D. Ramanan, “Multimodal object detection via bayesian fusion,” in *ECCV*, 2022.
- [46] X. Weng, Y. Wang, Y. Man, and K. M. Kitani, “GNN3DMOT: Graph neural network for 3d multi-object tracking with 2d-3d multi-feature learning,” in *IEEE/CVF CVPR*, 2020, pp. 6499–6508.
- [47] W. Zhang, H. Zhou, S. Sun, Z. Wang, J. Shi, and C. C. Loy, “Robust multi-modality multi-object tracking,” in *IEEE/CVF ICCV*, 2019.



APPENDIX I  
EQUIVALENT PENALTY FORM

We show step-by-step derivations leading to an equivalent penalty form of problem (4), repeated below for convenience

$$\begin{aligned} & \underset{U \in \{0,1\}^{m \times m}}{\text{minimize}} && \|UU^\top - S\|_F^2 && \text{(cycle consistency)} \\ & \text{subject to} && U \mathbf{1}_m = \mathbf{1}_m && \text{(one-to-one constraint)} \\ & && U_i^\top \mathbf{1}_{m_i} \leq \mathbf{1}_m && \text{(distinctness constraint)} \end{aligned}$$

**Equivalent problem.** From the definition of Frobenius norm, the objective of (4) can be expanded and simplified as

$$\begin{aligned} \|UU^\top - S\|_F^2 &= \langle UU^\top - S, UU^\top - S \rangle \\ &= \|UU^\top\|_F^2 - 2\langle UU^\top, S \rangle + \|S\|_F^2, \end{aligned} \quad (8)$$

where  $\langle A, B \rangle \stackrel{\text{def}}{=} \text{tr}(A^\top B) = \sum_{i,j} A_{ij} B_{ij}$  is the Frobenius inner product of matrices  $A$  and  $B$ . Further, it holds that

$$\|UU^\top\|_F^2 = \sum_{i,j} (UU^\top)_{ij}^2 = \sum_{i,j} (UU^\top)_{ij} = \langle UU^\top, \mathbf{1}_{m \times m} \rangle, \quad (9)$$

where the second equality follows by noting that entries of  $U$  are binary and therefore equal to their square. Combining (8) and (9), the objective can be written as

$$\|UU^\top - S\|_F^2 = \langle UU^\top, \mathbf{1}_{m \times m} - 2S \rangle + \|S\|_F^2. \quad (10)$$

Since  $S$  is given and is a constant of the optimization problem, the term  $\|S\|_F^2$  does not affect the solution and can be omitted from the objective. Thus, defining  $\bar{S} \stackrel{\text{def}}{=} \mathbf{1}_{m \times m} - 2S$ , problem (4) is equivalent to the following problem

$$\begin{aligned} & \underset{U \in \{0,1\}^{m \times m}}{\text{minimize}} && \langle UU^\top, \bar{S} \rangle && \text{(cycle consistency)} \\ & \text{subject to} && U \mathbf{1}_m = \mathbf{1}_m && \text{(one-to-one constraint)} \\ & && U_i^\top \mathbf{1}_{m_i} \leq \mathbf{1}_m && \text{(distinctness constraint)} \end{aligned} \quad (11)$$

**Penalty functions.** Toward deriving the proposed relaxation, we introduce the standard simplex and two penalty functions, allowing the reformulation of the constraints of (11) into an equivalent problem. With slight abuse of notation, the standard simplex defined for each row of a matrix is

$$\Delta^{m \times m} \stackrel{\text{def}}{=} \{U \in \mathbb{R}_+^{m \times m} : U \mathbf{1}_m = \mathbf{1}_m\}. \quad (12)$$

Observe that  $\Delta^{m \times m}$  captures the one-to-one constraint and that  $\{0,1\}^{m \times m} \subset \Delta^{m \times m}$ . Using the standard simplex, we first show that a binary  $U \in \Delta^{m \times m}$  must have orthogonal columns. This orthogonality property is *implicit* in the original formulation and we explicitly include it in the relaxation.

**Lemma 1.** *A matrix  $U \in \Delta^{m \times m}$  is binary if and only if the columns of  $U$  are orthogonal.*

*Proof.* Suppose, by contradiction, two columns  $v$  and  $w$  of  $U$  give  $\langle v, w \rangle \neq 0$ . Then, since  $U$  is binary, there exists at least one  $k \in \{1, \dots, m\}$  such that  $v_k = 1$  and  $w_k = 1$ . This implies that there are at least two 1 entries in the  $k$ 'th row of  $U$ . Consequently, the  $k$ -th row of vector  $U \mathbf{1}_m$  is strictly greater than 1, which violates the constraint  $U \mathbf{1}_m = \mathbf{1}_m$ .

Conversely, assume  $U \in \Delta^{m \times m}$  has orthogonal columns. Without loss of generality, we show that the first row of  $U$  is binary and, by applying a similar argument to other rows, we conclude that  $U$  is binary. Denote the first row of  $U$  by  $v_1$ . Because  $U \in \Delta^{m \times m}$ , there exists  $i \in \{1, \dots, m\}$  such that  $(v_1)_i > 0$ . Let  $u_i$  denote the  $i$ -th column of  $U$ . Orthogonality of columns implies that for all  $j \neq i$ ,

$$\begin{aligned} 0 &= u_i^\top u_j = \sum_{k=1}^m (u_i)_k (u_j)_k \\ &= (u_i)_1 (u_j)_1 + \sum_{k=2}^m (u_i)_k (u_j)_k \\ &= (v_1)_i (v_1)_j + \sum_{k=2}^m (u_i)_k (u_j)_k. \end{aligned} \quad (13)$$

Because  $U$  is non-negative, for (13) to hold we must have  $(v_1)_i (v_1)_j = 0$  for all  $j \neq i$ . Since  $(v_1)_i > 0$ , it follows that  $(v_1)_j = 0$  for all  $j \neq i$ . Further, since the sum of the entries of  $v_1$  is equal to 1, we have that  $(v_1)_i = 1$  so that the first row of  $U$  is binary.  $\square$

Because we seek binary  $U \in \Delta^{m \times m}$ , we introduce a penalty function corresponding to the column-wise orthogonality of  $U$ , defined as

$$\phi_{\text{orth}}(U) \stackrel{\text{def}}{=} \langle U^\top U, P_o \rangle, \quad (14)$$

where  $P_o \stackrel{\text{def}}{=} \mathbf{1}_{m \times m} - I_{m \times m}$ . Note that by definition,  $\langle U^\top U, P_o \rangle \stackrel{\text{def}}{=} \sum_{i,j} (U^\top U)_{ij} (P_o)_{ij} = \sum_{i \neq j} (U^\top U)_{ij}$ , which is the sum of non-diagonal entries. Therefore,  $\phi_{\text{orth}}(U) = 0$  if and only if the columns of  $U$  are orthogonal.

The second penalty function corresponds to the distinctness constraint and is defined as

$$\phi_{\text{dist}}(U) \stackrel{\text{def}}{=} \langle UU^\top, P_d \rangle, \quad (15)$$

where  $P_d \stackrel{\text{def}}{=} \text{blockdiag}(P_{d1}, \dots, P_{dn})$  and each  $m_i \times m_i$  matrix  $P_{di} \stackrel{\text{def}}{=} 2(\mathbf{1}_{m_i \times m_i} - I_{m_i \times m_i})$  ensures that the  $m_i$  observations of view  $i$  are distinct.

**Lemma 2.** *Given  $U \in \{0,1\}^{m \times m}$  and  $\phi_{\text{dist}}(U)$  as defined,  $\phi_{\text{dist}}(U) = 0$  if and only if  $U_i^\top \mathbf{1}_{m_i} \leq \mathbf{1}_m$ .*

*Proof.* Expanding  $\phi_{\text{dist}}(U)$  based on the  $n$  matrix blocks in  $U$  and  $P_d$  gives

$$\begin{aligned} \langle UU^\top, P_d \rangle &= \sum_{i=1}^n \langle U_i U_i^\top, P_{di} \rangle \\ &= \sum_{i=1}^n \langle U_i U_i^\top, \mathbf{1}_{m_i \times m_i} - I_{m_i \times m_i} \rangle \\ &= \sum_{i=1}^n \sum_{j \neq r} (U_i U_i^\top)_{jr}. \end{aligned} \quad (16)$$

Since  $U_i$  is binary, the latter summation is zero if and only if all matrices  $U_i U_i^\top$  are diagonal. Suppose  $\langle UU^\top, P_d \rangle = 0$  and, by contradiction, there exists  $U_i$  for which  $U_i U_i^\top$  is non-diagonal. This implies  $U_i$  has at least two non-orthogonal rows. From a similar proof-by-contradiction argument used

in the proof of Lemma 1 (based on rows instead of columns), non-orthogonality implies that there exists  $k$  such that the  $k$ -th elements of these two non-orthogonal rows are 1. Therefore, the  $k$ -th element of  $U_i^\top \mathbf{1}_{m_i}$  is strictly greater than 1, a contradiction. Now suppose  $U_i^\top \mathbf{1}_{m_i} \leq \mathbf{1}_m$ . Since  $U_i$  is binary, this implies that if the  $k$ -th element of a row of  $U_i$  is 1, then the  $k$ -th element of all other rows must be 0. Consequently, rows of  $U_i$  are orthogonal, which implies  $\sum_{j \neq r} (U_i U_i^\top)_{jr} = 0$  and therefore  $\langle U U^\top, P_d \rangle = 0$ .  $\square$

Using the standard simplex (12) and the penalty functions (14), (15), problem (11) can be equivalently expressed as problem (5), which is repeated below for convenience

$$\begin{aligned} & \underset{U}{\text{minimize}} && \langle U U^\top, \bar{S} \rangle && (\text{cycle consistency}) \\ & \text{subject to} && U \in \Delta^{m \times m} && (\text{one-to-one constraint}) \\ & && U \in \{0, 1\}^{m \times m} && (\text{binary constraint}) \\ & && \phi_{\text{orth}}(U) = 0 && (\text{orthogonality constraint}) \\ & && \phi_{\text{dist}}(U) = 0 && (\text{distinctness constraint}) \end{aligned}$$

## APPENDIX II THEORETICAL ANALYSIS

We present theoretical insights behind the relaxed problem (7) which lead to the MIXER algorithm. Consider the relaxation (7) in standard form [40], with  $\bar{S} \stackrel{\text{def}}{=} \mathbf{1} - 2S$

$$\begin{aligned} & \underset{U}{\text{minimize}} && F(U) \stackrel{\text{def}}{=} \langle U U^\top, \bar{S} \rangle \\ & && + d(\langle U^\top U, P_o \rangle + \langle U U^\top, P_d \rangle) \\ & \text{subject to} && U \geq \mathbf{0}_{m \times m} \\ & && U \mathbf{1}_m - \mathbf{1}_m = \mathbf{0}_m \end{aligned} \quad (17)$$

The Lagrangian of (17) is

$$\mathcal{L}(U; Y, \lambda) \stackrel{\text{def}}{=} F - \langle Y, U \rangle - \langle \lambda, U \mathbf{1}_m - \mathbf{1}_m \rangle, \quad (18)$$

where  $\lambda \in \mathbb{R}^m$  and  $Y \in \mathbb{R}^{m \times m}$  are the Lagrange multipliers for the equality and inequality constraints, respectively. From the first-order optimality conditions, stationary points  $U^* \in \Delta^{m \times m}$  of (17) must satisfy the KKT conditions

$$\nabla_U \mathcal{L} = \nabla F(U^*) - Y^* - \lambda^* \mathbf{1}_m^\top = 0, \quad (19a)$$

$$U^* \mathbf{1}_m - \mathbf{1}_m = \mathbf{0}_m, \quad (19b)$$

$$U_{ij}^* \geq 0, \quad \forall ij, \quad (19c)$$

$$Y_{ij}^* \geq 0, \quad \forall ij, \quad (19d)$$

$$Y_{ij}^* U_{ij}^* = 0, \quad \forall ij, \quad (19e)$$

where  $\nabla F(U) = 2\bar{S}U + 2d(U P_o + P_d U)$ .

The scalar  $d \geq 0$  controls the strength of the penalty functions and intuitively, pushes solutions of (17) towards binary, distinct solutions as it is increased. In this appendix, we first show results for  $d \rightarrow \infty$ , which effectively removes the data matrix  $\bar{S}$  from the objective of (17). After discussing how solutions of the relaxation (17) are guaranteed to converge to binary, feasible solutions with respect to the original problem (4) under the condition  $d \rightarrow \infty$ , we conclude by showing that these results hold for finite  $d$ . These results pave the way for our MIXER algorithm.

**Lemma 3.** *As  $d \rightarrow \infty$ , if a stationary point  $U^* \in \Delta^{m \times m}$  is binary, then  $\phi_{\text{dist}}(U^*) = 0$ , i.e., distinctness is satisfied.*

*Proof.* Without loss of generality, consider a single view, i.e.,  $n = 1$  and  $m = m_1$ . Therefore  $(P_d)_{ij} = 2(1 - \delta_{ij})$ , where  $\delta_{ij} = 1$  for  $i = j$  and 0 otherwise. By contradiction, suppose there exists a binary  $U^* \in \Delta^{m \times m}$  with at least one column  $k$  denoted  $u_k^*$  such that  $u_k^{*\top} \mathbf{1}_m = 1 + \rho > 1$  so that the distinctness constraint is violated. By stationarity (19a),

$$2\bar{S}U^* + 2d(U^* P_o + P_d U^*) - Y^* - \lambda^* \mathbf{1}_m^\top = 0. \quad (20)$$

Dividing (20) by  $2d$  and letting  $d \rightarrow \infty$  gives

$$U^* P_o + P_d U^* - Y^* - \lambda^* \mathbf{1}_m^\top = 0. \quad (21)$$

Consider the first row of (21). By definition of matrix multiplication we have the following terms

$$(U^* P_o)_{1j} = \sum_{i=1}^m U_{1i} (P_o)_{ij} = U_{1k} (P_o)_{kj} = 1 - \delta_{kj}, \quad (22)$$

$$\begin{aligned} (P_d U^*)_{1j} &= \sum_{i=1}^m (P_d)_{1i} U_{ij} = 2 \sum_{i=1}^m (1 - \delta_{1i}) U_{ij} \\ &= 2 \sum_{i=2}^m (1 - \delta_{1i}) U_{ij} = 2 \sum_{i=2}^m U_{ij} = 2\rho \delta_{kj}, \end{aligned} \quad (23)$$

so that the first row of (21) is

$$2(1 - \delta_{kj}) + 4\rho \delta_{kj} = Y_{1j}^* + \lambda_1^*. \quad (24)$$

Therefore, when  $j = k$ ,  $\lambda_1^* + Y_{1k}^* = 4\rho$  and since  $U_{1k}^* = 1$  by assumption,  $Y_{1k}^* = 0$  by complementarity (19e) so that  $\lambda_1^* = 4\rho$ . When  $j \neq k$ ,  $\lambda_1^* + Y_{1j}^* = 2$ , so that  $Y_{1j}^* = 2 - 4\rho < 0$ , a contradiction of dual feasibility (19d).  $\square$

From Lemma 3, we see that as  $d \rightarrow \infty$  there are no binary stationary points of (17) that violate distinctness.

The next result sheds light on the existence of *non-binary* stationary points of (17). Using this result, in combination with a framework to move in new descent directions when at a saddle point (we use [22]), we can easily detect and escape from non-binary saddle points.

**Proposition 1** ([22], [40]). *Given convex constraints  $\mathcal{C}$ , a stationary point  $x^* \in \mathcal{C}$  is a saddle point of the nonlinear problem  $\min_{x \in \mathcal{C}} f(x)$  if it satisfies the first-order necessary conditions and there are directions that are undecided to first order, but have negative curvature (i.e., will decrease the objective). That is, the following conditions must be satisfied*

- (i)  $\nabla f(x^*)^\top (x - x^*) \geq 0, \quad \forall x \in \mathcal{C}$ ,
- (ii)  $\exists y \in \mathcal{C}$  such that  $\nabla f(x^*)^\top (y - x^*) = 0$   
and  $(y - x^*)^\top \nabla^2 f(x^*) (y - x^*) < 0$ .

Let  $\text{vecr} : \mathbb{R}^{n \times m} \rightarrow \mathbb{R}^{nm}$  be the row-order vectorization operator that stacks matrix rows into a single column. Let  $u \stackrel{\text{def}}{=} \text{vecr}(U)$ , then the gradient of  $F(U)$  in (17) can be expressed as the vectorization

$$\nabla F_v(u) \stackrel{\text{def}}{=} 2(\bar{S} \otimes I)u + 2d(I \otimes P_o + P_d \otimes I)u. \quad (25)$$

**Lemma 4.** As  $d \rightarrow \infty$ , if a stationary point  $U^* \in \Delta^{m \times m}$  is non-binary, then  $U^*$  is a saddle point.

*Proof.* As  $d \rightarrow \infty$ , problem (17) is equivalent to a minimization over the same constraint manifold with the objective  $f(U) \stackrel{\text{def}}{=} \langle U^\top U, P_o \rangle + \langle UU^\top, P_d \rangle$  and vectorized gradient

$$\nabla f_v(u) \stackrel{\text{def}}{=} 2(I \otimes P_o + P_d \otimes I)u.$$

Let  $u^* \stackrel{\text{def}}{=} \text{vecr}(U^*)$  and assume that  $u^*$  has non-binary entries. Because  $\sum_j U_{ij}^* = 1 \forall i$ , there must be at least two non-zero elements  $a$  and  $b$  with  $0 < a \leq b < 1$ , so that  $u^* = [\dots, a, b, \dots]^\top$ . Take  $y = [\dots, a - \epsilon_a, b + \epsilon_b, \dots]^\top$  with  $\epsilon_a > 0, \epsilon_b > 0$  so that  $0 \leq a - \epsilon_a < b + \epsilon_b \leq 1$  and let  $v \stackrel{\text{def}}{=} y - u^* = [0, \dots, 0, -\epsilon_a, \epsilon_b, 0, \dots, 0]^\top$ . Observing that elements of  $\nabla f_v$  are non-negative, let the entries of  $\nabla f_v(u)$  be  $[\dots, c_a, c_b, \dots]^\top$ , where  $c_a \geq 0, c_b \geq 0$  and their placement corresponds to the non-zero elements of  $v$ . Then, let  $\epsilon_a = \epsilon/c_a$  and  $\epsilon_b = \epsilon/c_b$  with  $\epsilon > 0$  (or  $\epsilon_a = \epsilon$  if  $c_a = 0$  and similarly for  $\epsilon_b$ ). Therefore

$$\nabla f_v(u^*)^\top v = c_a \frac{-\epsilon}{c_a} + c_b \frac{\epsilon}{c_b} = 0.$$

Note that  $a, b$  are in the same row of  $U^*$ . Without loss of generality, suppose  $a, b$  where in the first two columns of the first row of  $U^*$ . Then,

$$\begin{aligned} v^\top \nabla^2 f_v(u^*) v &= 2v^\top (I \otimes P_o + P_d \otimes I) v \\ &= 2 \begin{bmatrix} -\epsilon_a \\ \epsilon_b \\ 0 \\ \vdots \end{bmatrix}^\top \begin{bmatrix} P_o & 2I & 2I & \cdots \\ 2I & P_o & 2I & \cdots \\ 2I & 2I & P_o & \cdots \\ \vdots & \vdots & \vdots & \ddots \end{bmatrix} \begin{bmatrix} -\epsilon_a \\ \epsilon_b \\ 0 \\ \vdots \end{bmatrix} \\ &= 2 \begin{bmatrix} -\epsilon_a \\ \epsilon_b \\ 0 \\ \vdots \end{bmatrix}^\top P_o \begin{bmatrix} -\epsilon_a \\ \epsilon_b \\ 0 \\ \vdots \end{bmatrix} = 2 \begin{bmatrix} -\epsilon_a \\ \epsilon_b \\ 0 \\ \vdots \end{bmatrix}^\top \begin{bmatrix} \epsilon_b \\ -\epsilon_a \\ * \\ \vdots \end{bmatrix} \\ &= 2(-\epsilon_a \epsilon_b - \epsilon_b \epsilon_a) = -4\epsilon_a \epsilon_b < 0. \end{aligned}$$

Therefore, the conditions of Proposition 1 are satisfied.  $\square$

**Lemma 5.** At a stationary point  $U^* \in \Delta^{m \times m}$  of (7), a non-zero element  $U_{ij}^* \neq 0$  has corresponding gradient  $\nabla F_{ij} = \sum_{k=1}^m (\nabla F \odot U^*)_{ik}$ . This implies that  $\nabla F_{ij} = \nabla F_{ik}$  for  $k \in \{k : U_{ik}^* \neq 0\}$ .

*Proof.* Considering the stationarity condition (19a), we can remove the dependence on  $Y$  by element-wise right multiplication of  $U$ . Because of complementarity (19e), we have

$$\nabla F \odot U - \lambda \mathbf{1}^\top \odot U = 0. \quad (26)$$

Noting that  $(\lambda \mathbf{1}^\top \odot U) \mathbf{1} = \lambda$ , multiplying on the right by  $\mathbf{1}$  and isolating  $\lambda$  yields

$$\lambda = (\nabla F \odot U) \mathbf{1} \quad (27)$$

Our aim is to eliminate explicit dependence of  $\lambda$  from (26). Substituting (27) into (26) yields

$$\begin{aligned} \nabla F \odot U - (\nabla F \odot U) \mathbf{1} \mathbf{1}^\top \odot U &= 0 \\ (\nabla F - (\nabla F \odot U) \mathbf{1}_{m \times m}) \odot U &= 0, \end{aligned}$$

which implies the following two cases

$$\begin{cases} U_{ij}^* = 0 \\ (\nabla F - (\nabla F \odot U) \mathbf{1}_{m \times m})_{ij} = 0 \end{cases}$$

Through simplification, when  $U_{ij}^* \neq 0$  we have

$$\begin{aligned} \nabla F_{ij} &= ((\nabla F \odot U) \mathbf{1}_{m \times m})_{ij} \\ &= (\nabla F \odot U)_{i:} (\mathbf{1}_{m \times m})_{:j} \\ &= \sum_{k=1}^m (\nabla F \odot U^*)_{ik}. \end{aligned} \quad (28)$$

Thus, on row  $i$ , for any  $j$  such that  $U_{ij}^* \neq 0$  we have that the corresponding  $\nabla F_{ij}$  is equal to (28) and therefore, all such  $\nabla F_{ij}$  on row  $i$  are equal.  $\square$

**Theorem 1.** If  $d \geq m + 1$ , then local minima are binary.

*Proof.* Let  $U \in \Delta^{m \times m}$  be a local minimum of the relaxed problem (7) with finite  $d$  and let  $U^* \in \{0, 1\}^{m \times m}$  be a local minimum of the relaxed problem (7) with  $d \rightarrow \infty$ . Then,  $\forall \epsilon > 0, \exists d^* > 0$  such that  $\forall d > d^*, \|U - U^*\|_{\max} \leq \epsilon$ , where  $\|A\|_{\max} \stackrel{\text{def}}{=} \max_{ij} |A_{ij}|$ . We prove two cases, first omitting the distinctness constraint and afterwards including it.

**Without distinctness.** By contradiction, assume  $d \geq m + 1$  and the local minimum  $U$  is not binary (i.e.,  $\|U - U^*\|_{\max} > \epsilon$ ). This implies that  $U$  has a non-binary row, which, without loss of generality, we denote by the  $i$ -th row

$$U_{i:} = [u_{i1} \quad u_{i2} \quad \cdots \quad u_{im'} \quad 0 \quad \cdots \quad 0].$$

Assuming that  $U_{i:}^* = [1 \quad 0 \quad \cdots \quad 0]$ , it must hold from  $\|U - U^*\|_{\max} < \epsilon$  that

$$\begin{aligned} 1 - \epsilon &\leq u_{i1} < 1 \\ 0 &< u_{ik} \leq \epsilon, \quad k = 2, 3, \dots, m'. \end{aligned} \quad (29)$$

From Lemma 5, we have that  $\nabla F_{i1} = \cdots = \nabla F_{im'}$ , and so, after dividing by  $2d$ , we have the system of  $m'$  equations

$$\begin{aligned} \frac{1}{2d} \nabla F_{i1} &= \frac{1}{d} \bar{S}_{i:} U_{:1} + U_{i:} (P_o)_{:1} + (P_d)_{i:} U_{:1} \\ &\vdots \\ \frac{1}{2d} \nabla F_{im'} &= \frac{1}{d} \bar{S}_{i:} U_{:m'} + U_{i:} (P_o)_{:m'} + (P_d)_{i:} U_{:m'}, \end{aligned}$$

which yields the following system by pairwise subtraction

$$\begin{aligned} u_{i1} - u_{i2} &= \frac{1}{d} \bar{S}_{i:} (U_{:1} - U_{:2}) + (P_d)_{i:} (U_{:1} - U_{:2}) \\ &\vdots \\ u_{i1} - u_{im'} &= \frac{1}{d} \bar{S}_{i:} (U_{:1} - U_{:m'}) + (P_d)_{i:} (U_{:1} - U_{:m'}). \end{aligned} \quad (30)$$

Ignoring the distinctness constraint (i.e., setting  $P_d := 0$ ), from (29), we have  $u_{i1} - u_{ik} \geq 1 - 2\epsilon$  and substitution gives

$$\frac{1}{d} |\bar{S}_{i:} (U_{:1} - U_{:k})| \geq 1 - 2\epsilon, \quad \forall k = 2, \dots, m'.$$

Since  $0 \leq U \leq 1$  and  $-1 \leq \bar{S} \leq 1$ , we have the bound

$$1 - 2\epsilon \leq \frac{1}{d} |\bar{S}_{i:}(U_{:1} - U_{:k})| \leq \frac{m}{d}, \quad \forall k = 2, \dots, m'.$$

Therefore,  $d \leq \frac{m}{1-2\epsilon}$  for  $0 < \epsilon < 0.5$ . Taking  $\epsilon \rightarrow 0$ , we have that  $d \leq m$ , which contradicts  $d > d^* \geq m + 1$ . Thus, no row of  $U$  can be non-binary.

**With distinctness.** Without loss of generality, assume that rows  $i$  to  $i + m''$  of  $U$  must satisfy distinctness. Therefore,

$$U_{i:i+m'',:}^* = \begin{bmatrix} 1 & 0 & \cdots & 0 & 0 & \cdots & 0 \\ 0 & 1 & \cdots & 0 & 0 & \cdots & 0 \\ & & \ddots & & & & \\ 0 & 0 & \cdots & 1 & 0 & \cdots & 0 \end{bmatrix}$$

By contradiction, assume  $d \geq m + 1$  and the local minimum  $U$  is not binary (i.e.,  $\|U - U^*\|_{\max} > \epsilon$ ). It follows that

$$U_{i:i+m'',:} = \begin{bmatrix} u_{i1} & \cdots & u_{im'} & 0 & \cdots & 0 \\ u_{i+1,1} & \cdots & u_{i+1,m'} & 0 & \cdots & 0 \\ & & \ddots & & & \\ u_{i+m'',1} & \cdots & u_{i+m'',m'} & 0 & \cdots & 0 \end{bmatrix}$$

with

$$\begin{aligned} 1 - \epsilon &\leq u_{i1}, u_{i+1,2}, \dots, u_{i+m'',m'} < 1 \\ 0 &< u_{i2}, u_{i3}, \dots, u_{im'} \leq \epsilon \\ 0 &< u_{i+1,1}, u_{i+1,3}, \dots, u_{im'} \leq \epsilon \\ &\vdots \\ 0 &< u_{i+m'',1}, u_{i+1,3}, \dots, u_{i+m'',m'-1} \leq \epsilon. \end{aligned} \quad (31)$$

Leveraging the structure of  $P_d$ , (30) can be simplified as

$$\begin{aligned} u_{i1} - u_{i2} &= \frac{1}{d} \bar{S}_{i:}(U_{:1} - U_{:2}) + 2(u_{i+1,1} - u_{i+1,2}) \\ &\quad + \cdots + 2(u_{i+m'',1} - u_{i+m'',2}) \\ &\quad \vdots \\ u_{i1} - u_{i2} &= \frac{1}{d} \bar{S}_{i:}(U_{:1} - U_{:2}) + 2(u_{i+1,1} - u_{i+1,m'}) \\ &\quad + \cdots + 2(u_{i+m'',1} - u_{i+m'',m'}). \end{aligned} \quad (32)$$

Rearranging terms of the first equation of (32) gives

$$(u_{i1} - u_{i2}) + 2(u_{i+1,2} - u_{i+1,1}) + \cdots + 2(u_{i+m'',2} - u_{i+m'',1}) = \frac{1}{d} \bar{S}_{i:}(U_{:1} - U_{:2}), \quad (33)$$

and similarly for the others. From (31), it follows that (33) is bounded by

$$\begin{aligned} \text{l.h.s (33)} &\geq 1 - 2\epsilon + 2(1 - 2\epsilon) - 2\epsilon - \cdots - 2\epsilon = 3 - (2m'' + 4)\epsilon \\ \text{r.h.s (33)} &\leq \frac{m}{d}, \end{aligned}$$

implying that  $d \leq \frac{m}{3-(2m''+4)\epsilon}$  for  $0 < \epsilon < \frac{3}{2m''+4}$ . Taking  $\epsilon \rightarrow 0$ , we have  $d \leq \frac{m}{3}$ , which contradicts  $d > d^* \geq m + 1$ . Thus, no row of  $U$  can be non-binary.  $\square$